HHS Public Access

Author manuscript

Histol Histopathol. Author manuscript; available in PMC 2018 March 01.

Published in final edited form as:

Histol Histopathol. 2015 May ; 30(5): 559–568. doi:10.14670/HH-30.559.

Lymphoid hyperplasia and lymphoma in KSHV K1 transgenic mice

Zuzana Berkova[1], **Shu Wang**[1], **Lalit Sehgal**[1], **Keyur Pravinchandra Patel**[2], **Om Prakash**[3], and **Felipe Samaniego**[1]

[1]Department of Lymphoma and Myeloma, The University of Texas MD Anderson Cancer Center, Houston, TX

[2]Department of Hematopathology, The University of Texas MD Anderson Cancer Center, Houston, TX

[3]Laboratory of Molecular Oncology and Department of Pathology, Ochsner Clinic Foundation, New Orleans, LA

Abstract

Growing evidence supports the involvement of human herpervirus 8, Kaposi's sarcoma associated herpesvirus (KSHV), in the pathology of primary effusion lymphoma, multicentric Castleman's disease, and Kaposi's sarcoma, but the exact mechanism of KSHV contribution to the oncogenic process remains elusive.

We studied transgenic mice expressing the ORF K1 of KSHV, whose position in the KSHV genome corresponds to known lymphoproliferative genes of other herpesviruses. K1 protein was previously shown to contain a constitutively active ITAM domain, involved in activation of Akt and pro-survival signaling, and to inhibit Fas-mediated apoptosis by interfering with binding of FasL. All this pointed to a possible role of K1 in the pathogenesis of KSHV-associated cancers.

K1 transgenic mice (80–90%) developed lymphoid hyperplasia and splenomegaly at 8 and 10 months of age, 25% had confirmed diagnosis of lymphoma, and 50% developed abdominal and/or hepatic tumors by 18 months of age. Histological examination showed loss of splenic architecture and increased cellularity. Lymph nodes showed disrupted architecture with effaced follicles and other pathological changes, including signs of angiofollicular lymphoid hyperplasia. One of the livers showed signs of angiosarcoma.

In summary, our histology results revealed pathological changes in K1 transgenic mice similar to lymphoma, Castleman's disease, and angiosarcoma, suggesting that K1 may contribute to the development of KSHV-associated cancers.

Keywords

KSHV K1; ITAM; lymphoma; Fas receptor; apoptosis

Correspondence should be addressed to: Dr. Felipe Samaniego, The University of Texas – MD Anderson Cancer Center, Department of Lymphoma and Myeloma, 1515 Holcombe Blvd. Unit #429, Houston, TX 77030, USA; fsamaniego@mdanderson.org.

INTRODUCTION

Human herpesvirus 8, better known as Kaposi's sarcoma-associated herpesvirus (KSHV), infects B-lymphocytes and endothelial cells. In addition to Kaposi's sarcoma (KS), a neoplasm of endothelial cells, KSHV infection of B-cells leads to B-lymphoproliferative diseases, primary effusion lymphoma (PEL) and multicentric Castleman's disease (MCD) (Edelman 2005).

Our attention attracted ORF K1 of KSHV, which encodes a 46 kDa transmembrane glycoprotein K1 and corresponds to genomic positions of lymphoproliferative genes of other herpesviruses such as EBV and herpesvirus saimiri (Nicholas et al. 1998). K1 protein expression during lytic phase of KSHV infection was well shown and is widely accepted, but K1 expression during latent infection remained uncertain mainly due to a lack of reliable detection methods/antibodies. However, low level of K1 expression was recently detected in latently infected cells (Wang et al. 2006; Chandriani and Ganem 2010) underscoring the possibility of K1 involvement in induction of KS, PEL, and MCD.

Expression of K1 transforms rodent fibroblasts (Lee et al. 1998), activates Akt signaling (Tomlinson and Damania 2004; Wen and Damania 2010), and blocks apoptosis (Wang et al. 2006). Expression of K1 in endothelial cells increases production and secretion of vascular endothelial growth factor (VEGF), and activates prosurvival Akt signaling leading to immortalization of endothelial cells and thus, could have a key role in tumorigenesis of KS (Wang et al. 2006).

The focus of our investigation is on the contribution of K1 to lymphoproliferation and development of PEL and Castleman's disease. We and others had shown previously that expression of K1 in lymphocytes activates kinases Syk and Lyn as well as NF-κB pathway (Lagunoff et al. 1999; Prakash et al. 2002; Prakash et al. 2005), and both of those effects depend on K1 cytoplasmic ITAM motif. In addition, it was shown that K1 inhibits Fas apoptotic signaling (Tomlinson and Damania 2004; Wang et al. 2007; Wen and Damania 2010). This effect is mediated at least in part by the binding of K1 extracellular immunoglobulin-like domain to Fas receptor and interfering with binding of FasL, independently of the ITAM (Berkova et al. 2009). Fas-mediated apoptosis is important for proper development of B-cells and their homeostasis, and it is especially critical in germinal center (GC) B-cells where inhibition of Fas alone leads to lymphoproliferation (Hao et al. 2008). In this work, we aimed to show the effects of K1 expression on lymphoproliferation and apoptosis in mice.

MATERIALS AND METHODS

K1 transgenic mice

Production of heterozygous mouse lines expressing K1 (subtype C3) under the SV40 promoter was previously described (Prakash et al. 2002). Heterozygous males were crossed with C57BL/6 females to obtain K1+/− and K1−/− progeny mice for comparative analysis. Genomic DNA was isolated from tail clippings using DNeasy Tissue Kit (Qiagen, Valencia, CA) and used as a template for PCR amplification of K1 [5′-

ATGTTCCTGTATGTTGTCTGC-3′ and 5′-ACTAAGCTATTAGTACTGAATGT-3′] to establish K1 status of the progeny. Mouse beta-globin primers [5′ CCAATCTGCTCACACAGGATAGAGAGGGCAGG 3′ and 5′ CCTTGAGGCTGTCCAAGTGATTCAGGCCATCG 3′] were used as amplification control. Animal care and use was in compliance with the MD Anderson Cancer Center Institutional Animal Care and Use Committee guidelines.

Histology, immunohistochemistry, and pathology evaluation

Mice were sacrificed at indicated age, and necropsy examination was performed, which included gross examination of the size of lymph nodes, spleen, and the presence of tumors masses. Spleens were harvested and weighted. Thymuses, lymph nodes, and any tumors or tissues with abnormal appearance were also harvested immediately after sacrifice. All harvested tissues were frozen or fixed in 10% buffered formalin and embedded in paraffin. For histological evaluation, 5 micro-meter thick formalin fixed paraffin embedded sections were treated with an unmasking kit (Vector Laboratories, Burlingame, CA) and stained with hematoxylin and eosin (both from Fisher Scientific, Pittsburgh, PA). Expression of K1 was detected in unmasked sections by staining with mouse monoclonal K1 antibody 2H5 (kindly provided by Dr. J.U. Jung, University of Southern California, Los Angeles, CA) followed by Texas Red-conjugated goat anti-mouse IgG, and nuclei were stained with Hoechst 33342 (both from Life Technologies, Carlsbad, CA). Expression of B220, κ and λ light chains was detected by staining with anti-mouse B220 (R&D Systems, Minneapolis, MN), anti-mouse κ and λ light chain specific antibodies (both from Sigma Aldrich, St. Louis, MO), expression of Ki67 was detected with rat monoclonal anti-mouse Ki67 antibody (clone TEC-3; DAKO, Carpinteria, CA) and CXCR5 was detected with rabbit polyclonal antibody (EMD Millipore) followed by staining and developing using an ABC staining kit (Vector Laboratories).

Lymphoid hyperplasia was defined as the presence of the lymph node(s) larger than 3 mm and/or spleen weight larger than the mean weight ± 2 × SD of the spleens harvested from the age-matched K1-negative littermates. Lymphoma diagnosis was made based on the morphological changes observed in the lymph nodes and spleens.

Isolation of splenocytes and thymocytes, induction of apoptosis, flow cytometry, and qRT-PCR

Spleens and thymuses of 6 month old mice were homogenized in D-PBS into single-cell suspensions using cell strainer. Erythrocytes were lysed in ACK lysis buffer (GIBCO – Life Technologies, Carlsbad, CA) 10 minutes at room temperature. Remaining cells were counted and collected.

Cells were resuspended in RPMI medium supplemented with 10% fetal bovine serum (both from HyClone, Logan, UT), and aliquots of 1×10^6 cells per mL were incubated 50 ng/mL of agonistic anti-mouse Fas antibody Jo2 (BD Pharmingen, San Jose, CA) crosslinked with 2 μg/mL of protein G (Invitrogen– Life Technologies, Carlsbad, CA) to induce apoptosis. Cells were harvested at indicated times post induction, stained with Hoechst 33342, and analyzed for apoptosis by nuclear fragmentation.

Total cellular RNA was extracted from isolated splenocytes with RNeasy Mini Kit according to the manufacturer's instructions (Qiagen – SABiosciences, Germantown, MD). The first-strand cDNA was synthesized using a Superscript™ II reverse transcriptase kit (Invitrogen–Life Technologies, Carlsbad, CA) according to the manufacturer's protocol. Samples were analyzed on 96-well microtiter plates using the StepOnePlus™ Real-Time PCR Systems (Applied Biosystems - Life Technologies, Carlsbad, CA) with primers listed below using 40 cycles of 95°C for 15 seconds and 60°C for 1 minute and by SYBR green method for detection. qRT-PCR data were analyzed by the Step-One software version 2.1.

mIL6 F	5′-ACCAGAGGAAATTTTCAATAGGC-′3
mIL R	5′-TGATGCACTTGCAGAAAACA-′3
mCXCR5 F	5′-TCCTGTAGGGGAATCTCCGT-′3
mCXCR 5 R	5′-ACTAACCCTGGACATGGGC-′3
mL32 F	5′-GGCTTTTCGGTTCTTAGAGGA-′3
mL32 R	5′-TTCCTGGTCCACAATGTCAA-′3

Fas challenge and survival of K1 transgenic mice

Eight weeks old K1 transgenic mice were challenged by intraperitoneal administration of agonistic Fas antibody Jo2 (0.4 μg/g weight; BD Pharmingen, San Jose, CA) and monitored for survival up to 6 hours post challenge (Ogasawara et al. 1993; Berkova et al. 2009). The extent of hemorrhaging and increased vasculature (Fig. 2E) were evaluated in control mouse and K1 transgenic mouse #445 by two independent investigators using Adobe Photoshop. Total tissue areas shown in Figure 2E (4x) and the corresponding areas representing blood vessels or hemorrhaging were manually outlined and converted to pixels. The extent of hemorrhaging or vasculature was calculated from the ratio of corresponding pixels to the number of pixels representing the whole tissue and expressed as percentage of the tissue area. The standard deviation represents variability between independent measurements.

Statistical evaluation

Comparisons between groups were carried out using Student's *t* test. Two-sided P-values < 0.05 were considered to be statistically significant.

RESULTS

Lymphoid tumors were detected in 18-month old K1 transgenic mice

K1 transgenic mice and their K1-negative littermates were sacrificed at 18 months of age and analyzed for lymphoid hyperplasia and the evidence of cancer.

Seven out of 8 K1 transgenic mice (87.5 %) showed signs of lymphoid hyperplasia in the form of enlarged lymph nodes (defined as more than 3 mm in diameter) and/or splenomegaly (average spleen weight was 301 mg, ranging from 80 to 1000 mg). Histological examination of spleens revealed disrupted architecture (Fig. 1A) in 3 mice and the presence of large atypical cells (Table 1; # 428, # 429, #437). Surprisingly, the largest spleen (# 437; 1000 mg) showed morphologic findings suspicious for but not definitive for lymphoma - loss of separation of white and red pulp and presence of large atypical cells

(Table 1). Lymph nodes of all 7 mice showed disrupted architecture with effaced follicles and other pathological changes illustrated in Fig. 1B and summarized in Table 1. Notable were changes in the enlarged lymph nodes of mice # 414 and # 445 (Fig. 1B); increased vasculature with perivascular lymphoid sheets surrounded by plasma cells indicative of angiofollicular lymphoid hyperplasia. Lymph nodes of mice #437 showed effaced architecture and increased interfollicular plasma cell numbers, morphologically resembling plasma cell variant Castleman's disease (Fig. 1B).

Four out of those 7 mice developed also abdominal or hepatic lesions (Fig. 2A), majority of which were consistent with cysts or abscesses (Table 1). One of the mice (# 428) had mesenteric mass as well as masses on the liver and the adrenal glands (Fig. 2B). Histological examination and B220 staining of mesenteric and adrenal masses revealed B220-positive lymphoid tissue with no architecture, uniform cells population with occasional characteristic large atypical lymphocytes showing irregular nuclei/prominent nucleoli, vesicular chromatin, numerous mitotic cells, and frequent apoptosis (Fig. 2C). This finding together with the extent of the morphological changes in the spleen and lymph nodes (Table 1 and Fig. 1) confirmed diagnosis of multifocal lymphoma. A closer examination of the mesenteric mass from mouse # 429 revealed a grossly enlarged lymph node with B220-positive follicles (Fig. 2D). Tightly packed back-to-back follicles (Fig. 2D; 20x) separated by sheets of plasma cells (Fig. 2D; 40x) indicated B-cell lymphoma with a nodular pattern/follicular lymphoma. One of the livers (# 445) showed regions with an abnormal appearance (Fig. 2E). At closer histological examination of those regions, we observed hemorrhaging expanding to over 14.2 ± 1.3% of the tissue section area, increased vasculature compared to control mice (6.4 ± 0.5% vs. 1.5 ± 0.5 % of the tissue area; $P < 0.004$), and dividing spindle-like cells (Fig. 2E; 40x), all consistent with some of the morphological characteristics of angiosarcoma. None of the 4 K1-negative littermates showed enlarged lymphoid organs, masses in the abdominal and thoracic cavities, or any other gross abnormalities.

K1 transgenic mice develop lymphoid hyperplasia and splenomegaly at 8 to 10 months of age

To learn more about the time-course of the development of lymphoid hyperplasia, we sacrificed a second group of K1 transgenic mice and their littermates at 8 months of age. Nine out of 10 K1 mice (90%), but none of the 5 control mice, had enlarged cervical lymph nodes (larger than 3 mm), thymus, and apparently enlarged Payer's patches (Fig. 3A–C). An additional group of five K1 transgenic mice and six K1-negative littermates were sacrificed at 10 months. At this age, 4 out of 5 (80%) K1 transgenic mice but none of the control mice had enlarged spleens [weight larger than average plus 2 × SD of control spleens] (Fig. 3D). The average weight of K1 spleens was significantly higher than weight of control spleens (332 ± 200 mg vs. 94 ± 26 mg; P-value < 0.03).

Histological analysis of spleens confirmed previously observed increased cellularity (Fig. 1A) and a complete loss of splenic architecture (Fig. 4A). Interestingly, there were no significant differences in staining for proliferation marker Ki67 between control and K1 spleens (data not shown) suggesting that increased cellularity was not caused by increased cell proliferation. Immunohistochemical staining confirmed the expression of K1 in spleens.

B-cell lymphomas are characterized by altered kappa:lambda light chain ratio (Chizuka et al. 2002). Thus, we stained spleen sections with kappa:lambda light chain-specific antibodies. Foci of kappa-light chain positive B-cells were present, but only scattered single cells stained positive for lambda-light chains (Fig. 4A). However, the observed high kappa:lambda light chain ratio is considered normal for mouse tissues.

Elevated levels of IL-6 are often observed in HHV-8 related lymphomas (Hengge et al. 2002). We thus analyzed expression of IL-6 mRNA in control and K1 splenocytes by qRT-PCR. As shown in figure 4B (left panel), K1 splenocytes expressed higher levels of IL-6 mRNA; 6 out of 7 K1 samples had levels if IL-6 more than 2-fold higher than controls.

CXCR5 is a chemokine receptor responsible for homing of B1 cells into peritoneum and its expression is mediated by Oct-2, one of the K1 target genes. In our K1 transgenic mouse our model, no differences in the expression of CXCR5 were detected in spleen sections by immunohistochemistry (data not shown), but 5 out of 7 samples of K1 transgenic splenocytes showed elevated levels of CXCR5 mRNA (range 1.11–1.90) (Fig. 4B – right panel).

Splenocytes and thymocytes of K1 transgenic mice are resistant to Fas-mediated apoptosis

Our previous work showed that K1 blocks Fas signaling by direct binding of Fas and prevention of FasL binding (Wang et al. 2007; Berkova et al. 2009). Not surprisingly, the observed loss of normal splenic architecture and expansion of B-cell and T-cell populations in the enlarged spleens were reminiscent of the effects observed in Fas-deficient mice (Hao et al. 2008). To prove that disruption of Fas signaling by K1 expression in our transgenic mice precedes and possibly contributes to lymphoid hyperplasia and splenomegaly, we isolated splenocytes and thymocytes from 6 month old mice and tested their responses to Fas activation. As expected, responses of splenocytes from K1 transgenic mice to Fas activation were blunted when compared with control littermates, and differences were statistically significant at all treatment time-points tested (Fig. 4C). Thymocytes were similarly resistant to FasL-induced apoptosis (42% vs. 92% of apoptosis after 16 hours of treatment or data not shown).

Liver is a tissue that is highly susceptible to Fas stimulation (Ogasawara et al. 1993). To further confirm functionality of K1 transgene in the Fas apoptotic pathway, we challenged twelve 8-week-old K1 transgenic mice and 22 of their K1-negative littermates with a lethal dose of agonistic Fas antibody Jo2 and monitored their survival up to 6 hours post-challenge (Ogasawara et al. 1993; Wang et al. 2007; Berkova et al. 2009). As expected, 9 out of 12 (75%) K1 mice survived the challenge, whereas a majority (13 of 22) of K1-negative littermates died within the observation period ($P < 0.05$) (Fig. 4D).

DISCUSSION

The K1 protein of KSHV was previously shown to bind Fas and block Fas-mediated apoptosis (Tomlinson and Damania 2004; Wang et al. 2007; Berkova et al. 2009; Wen and Damania 2010) in addition to activation of Lyn kinase, NF-κB pathway, and upregulation of

Oct-2 (Prakash et al. 2002; Prakash et al. 2005). In this study, we show that the expression of a single allele of K1 transgene is sufficient to profoundly affect primarily the lymphatic system and emulates the development of KSHV-associated pathologies; angiosarcoma, angiofollicular lymphoid hyperplasia, and lymphoma.

K1 was shown to activate kinases Syk (Lagunoff et al. 1999) and Lyn (Prakash et al. 2002) via its constitutively active ITAM (Lee et al. 1998). However, we had shown previously that Lyn, not Syk, is active in B-lymphocytes and tumor tissues of K1 transgenic mice (Prakash et al. 2002). There are documented downstream effects of constitutive Lyn activation in K1 transgenic mice - nuclear translocation of NF-κB with the subsequent expression of angiogenic factors bFGF and VEGF (Prakash et al. 2002; Prakash et al. 2005). In line with this finding, we observed increased vascularity in lymph nodes of two K1 transgenic mice (# 414, # 445 in Fig. 2A), suggesting angiofollicular lymphoid hyperplasia, and in the liver of one of those mice (# 445), which also showed a region with spindle-like cells indicative of angiosarcoma (Fig. 2E). Interestingly, these two mice showed lymphoid hyperplasia but no signs of lymphoma (Table 1). While upregulated Lyn activity is strongly associated with lymphoma/leukemia and their prognosis, upregulated Lyn activity alone appears insufficient to induce lymphoma/leukemia; reviewed by Evan Ingley (Ingley 2012). On the contrary, mouse models with Lyn gain of function show significantly decreased number of $B220^+$ B-cells in blood, bone marrow, lymph nodes, and spleens (Hibbs et al. 2002). However, our results suggest that K1 ITAM-mediated activation of Lyn can induce angiogenesis and development of angiosarcoma and angiofollicular lymphoid hyperplasia that points to a possible contribution of K1 to the development of Kaposi's sarcoma and KSHV-associated multicentric Castleman's disease. Constitutive activation of NF-κB in K1 transgenic mice also elevates B-cell specific transcriptional factor Oct-2 (Prakash et al. 2002), which upregulates expression of CXCR5, a chemokine receptor responsible for homing of B1 cells into peritoneum (Pevzner et al. 1999), and can thus contribute to primary effusion lymphoma. In our K1 transgenic mouse our model, 5 out of 7 samples of K1 transgenic splenocytes showed elevated levels of CXCR5 mRNA.

In addition to K1 ITAM-mediated activation of Lyn kinase and NF-κB pathway, K1 was also shown to bind to Fas via its Ig-like domain and disable Fas signaling by interference with FasL binding (Berkova et al. 2009). We confirmed that apoptotic responses to FasL stimulation are significantly blunted in splenocytes (Fig. 4B) and thymocytes of K1 transgenic mice. Lymphoid hyperplasia and lymphoproliferative autoimmune disorders are commonly observed in Fas-disabled *Lpr* mice as well as in $fas^{del/del}$ mice and in mice with T-cell and B-cell specific ablation of Fas (Adachi et al. 1996; Hao et al. 2004; Hao et al. 2008). The lymphoid hyperplasia and loss of architecture of the lymph nodes and spleens of K1 transgenic mice (Fig. 2) resemble those in *Lpr*, $fas^{del/del}$ mice as well as in $fas^{fl/lpr}$ CD-4-*cre* mice with specific inactivation of Fas in T-cells. However, the hallmark of disorder in those mice, the presence of abnormal $B220^+Thy1.2^+$ cells (DN T-cells), is absent in K1 transgenic mice. In this regard, K1 transgenic mice resemble more the $fas^{fl/lpr}$ CD-19-*cre* mice with specific inactivation of Fas in B-cells (Hao et al. 2008). The KSHV infects primarily B-cells and endothelial cells, and thus one would expect that KSHV encoded proteins have evolved to target specifically signaling pathways in those cell types.

In conclusion, our data show that a single allele of K1 is sufficient to induce a wide range of pathological disturbances: angiosarcoma, angiofollicular lymphoid hyperplasia, and lymphoma, resembling the KSHV-associated pathologies (Edelman 2005). Despite the fact that K1 was expressed under a ubiquitous SV40 promoter in all mouse tissues, the observed pathologies were limited to the lymphatic system and only one mouse showed pathology in the liver, both tissues that are exquisitely sensitive to Fas. This finding also correlates with KSHV behavior, associated diseases of whose are limited to the lymphatic system despite a rather wide cell tropism of KSHV in vitro and in vivo (Naranatt et al. 2004).

References

Adachi M, Suematsu S, Suda T, Watanabe D, Fukuyama H, Ogasawara J, Tanaka T, Yoshida N, Nagata S. Enhanced and accelerated lymphoproliferation in Fas-null mice. Proc Natl Acad Sci U S A. 1996; 93:2131–2136. [PubMed: 8700897]

Berkova Z, Wang S, Wise JF, Maeng H, Ji Y, Samaniego F. Mechanism of Fas signaling regulation by human herpesvirus 8 K1 oncoprotein. J Natl Cancer Inst. 2009; 101:399–411. [PubMed: 19276446]

Chandriani S, Ganem D. Array-based transcript profiling and limiting-dilution reverse transcription-PCR analysis identify additional latent genes in Kaposi's sarcoma-associated herpesvirus. J Virol. 2010; 84:5565–5573. [PubMed: 20219929]

Chizuka A, Kanda Y, Nannya Y, Oshima K, Kaneko M, Yamamoto R, Suguro M, Hamaki T, Matsuyama T, Takezako N. The diagnostic value of kappa/lambda ratios determined by flow cytometric analysis of biopsy specimens in B-cell lymphoma. Clin Lab Haematol. 2002; 24:33–36. [PubMed: 11843896]

Edelman DC. Human herpesvirus 8–a novel human pathogen. Virol J. 2005; 2:78. [PubMed: 16138925]

Hao Z, Duncan GS, Seagal J, Su YW, Hong C, Haight J, Chen NJ, Elia A, Wakeham A, Li WY. Fas receptor expression in germinal-center B cells is essential for T and B lymphocyte homeostasis. Immunity. 2008; 29:615–627. [PubMed: 18835195]

Hao Z, Hampel B, Yagita H, Rajewsky K. T cell-specific ablation of Fas leads to Fas ligand-mediated lymphocyte depletion and inflammatory pulmonary fibrosis. J Exp Med. 2004; 199:1355–1365. [PubMed: 15148335]

Hengge UR, Ruzicka T, Tyring SK, Stuschke M, Roggendorf M, Schwartz RA, Seeber S. Update on Kaposi's sarcoma and other HHV8 associated diseases. Part 2: pathogenesis, Castleman's disease, and pleural effusion lymphoma. Lancet Infect Dis. 2002; 2:344–352. [PubMed: 12144897]

Hibbs ML, Harder KW, Armes J, Kountouri N, Quilici C, Casagranda F, Dunn AR, Tarlinton DM. Sustained activation of Lyn tyrosine kinase in vivo leads to autoimmunity. J Exp Med. 2002; 196:1593–1604. [PubMed: 12486102]

Ingley E. Functions of the Lyn tyrosine kinase in health and disease. Cell Commun Signal. 2012; 10:21. [PubMed: 22805580]

Lagunoff M, Majeti R, Weiss A, Ganem D. Deregulated signal transduction by the K1 gene product of Kaposi's sarcoma-associated herpesvirus. Proc Natl Acad Sci U S A. 1999; 96:5704–5709. [PubMed: 10318948]

Lee H, Veazey R, Williams K, Li M, Guo J, Neipel F, Fleckenstein B, Lackner A, Desrosiers RC, Jung JU. Deregulation of cell growth by the K1 gene of Kaposi's sarcoma-associated herpesvirus. Nat Med. 1998; 4:435–440. [PubMed: 9546789]

Naranatt PP, Krishnan HH, Svojanovsky SR, Bloomer C, Mathur S, Chandran B. Host gene induction and transcriptional reprogramming in Kaposi's sarcoma-associated herpesvirus (KSHV/HHV-8)-infected endothelial, fibroblast, and B cells: insights into modulation events early during infection. Cancer Res. 2004; 64:72–84. [PubMed: 14729610]

Nicholas J, Zong JC, Alcendor DJ, Ciufo DM, Poole LJ, Sarisky RT, Chiou CJ, Zhang X, Wan X, Guo HG. Novel organizational features, captured cellular genes, and strain variability within the genome of KSHV/HHV8. J Natl Cancer Inst Monogr. 1998:79–88. [PubMed: 9709308]

Ogasawara J, Watanabe-Fukunaga R, Adachi M, Matsuzawa A, Kasugai T, Kitamura Y, Itoh N, Suda T, Nagata S. Lethal effect of the anti-Fas antibody in mice. Nature. 1993; 364:806–809. [PubMed: 7689176]

Pevzner V, Wolf I, Burgstahler R, Forster R, Lipp M. Regulation of expression of chemokine receptor BLR1/CXCR5 during B cell maturation. Curr Top Microbiol Immunol. 1999; 246:79–84. [PubMed: 10396042]

Prakash O, Swamy OR, Peng X, Tang ZY, Li L, Larson JE, Cohen JC, Gill J, Farr G, Wang S, Samaniego F. Activation of Src kinase Lyn by the Kaposi sarcoma-associated herpesvirus K1 protein: implications for lymphomagenesis. Blood. 2005; 105:3987–3994. [PubMed: 15665117]

Prakash O, Tang ZY, Peng X, Coleman R, Gill J, Farr G, Samaniego F. Tumorigenesis and aberrant signaling in transgenic mice expressing the human herpesvirus-8 K1 gene. J Natl Cancer Inst. 2002; 94:926–935. [PubMed: 12072546]

Tomlinson CC, Damania B. The K1 protein of Kaposi's sarcoma-associated herpesvirus activates the Akt signaling pathway. J Virol. 2004; 78:1918–1927. [PubMed: 14747556]

Wang L, Dittmer DP, Tomlinson CC, Fakhari FD, Damania B. Immortalization of primary endothelial cells by the K1 protein of Kaposi's sarcoma-associated herpesvirus. Cancer Res. 2006; 66:3658–3666. [PubMed: 16585191]

Wang S, Maeng H, Young DP, Prakash O, Fayad LE, Younes A, Samaniego F. K1 protein of human herpesvirus 8 suppresses lymphoma cell Fas-mediated apoptosis. Blood. 2007; 109:2174–2182. [PubMed: 17090655]

Wen KW, Damania B. Hsp90 and Hsp40/Erdj3 are required for the expression and anti-apoptotic function of KSHV K1. Oncogene. 2010; 29:3532–3544. [PubMed: 20418907]

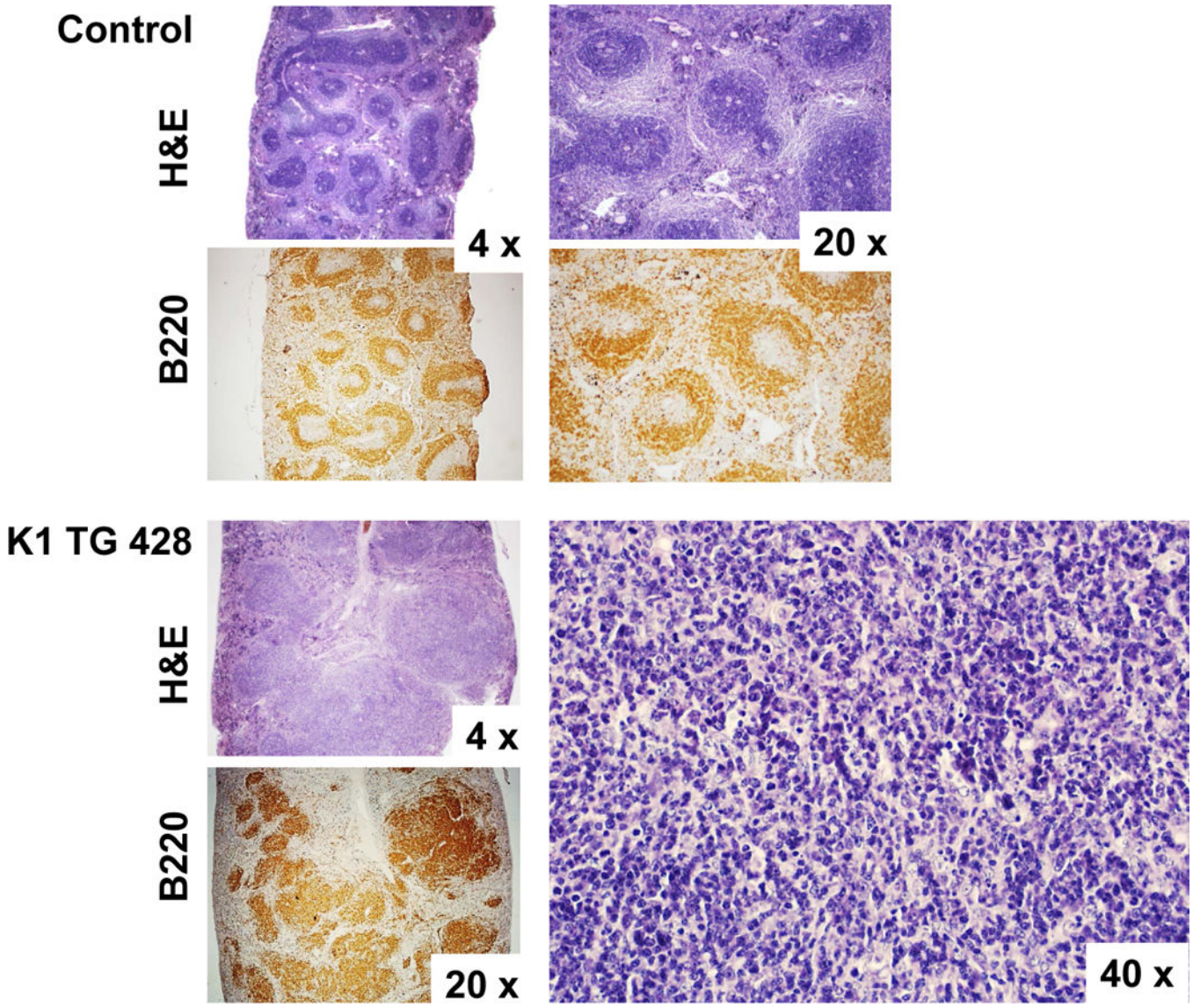

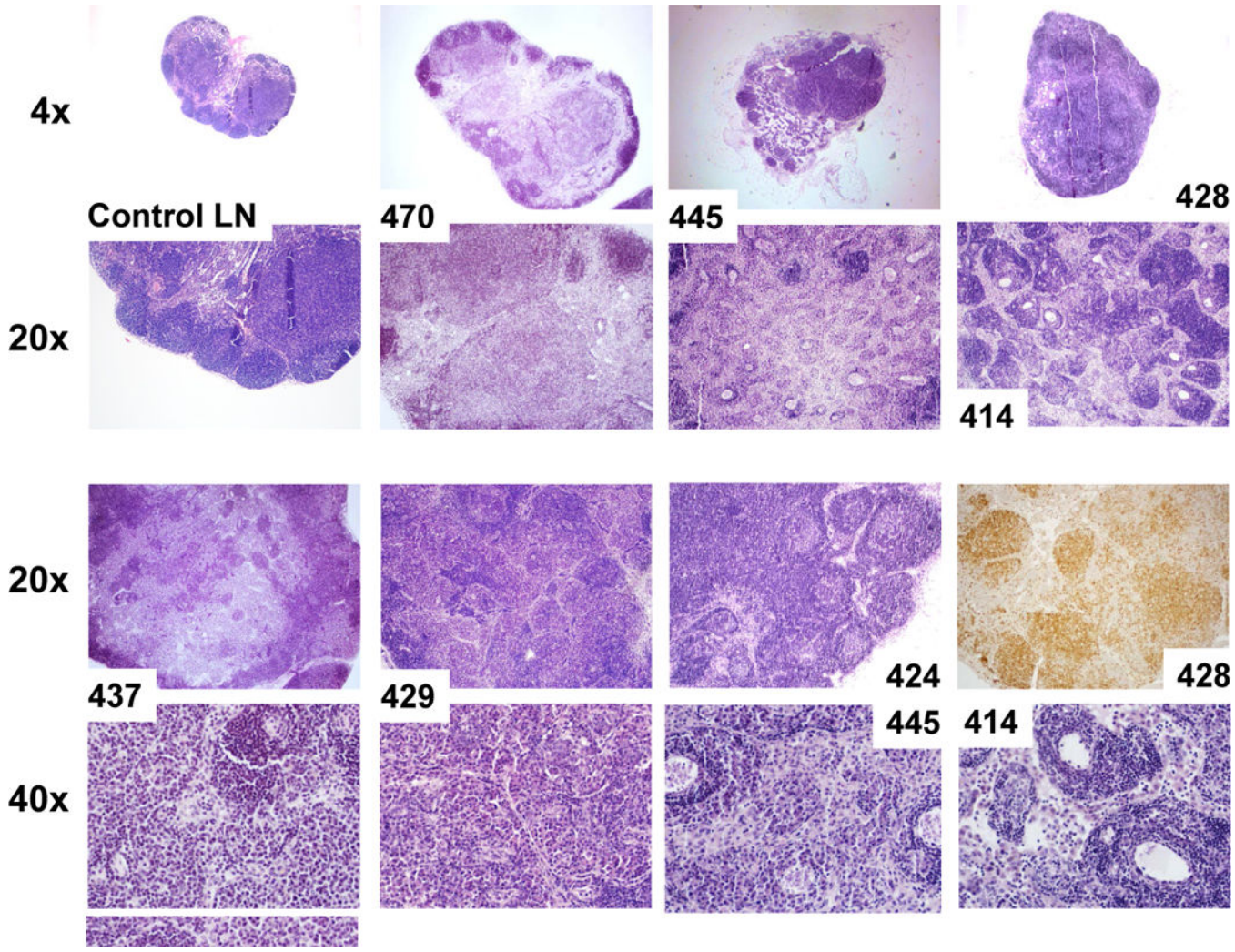

Figure 1. Disrupted splenic and lymph node architecture in 18 month old K1 transgenic mice

(A) Hematoxylin/eosin (H&E) and B-cell marker (B220) stained spleens of control (K1-negative littermate) and K1 transgenic mouse # 428; **(B)** H&E stained lymph nodes of control mouse and seven mice with lymphoid hyperplasia. 20x image of # 428 shows staining with B-cell marker B220.

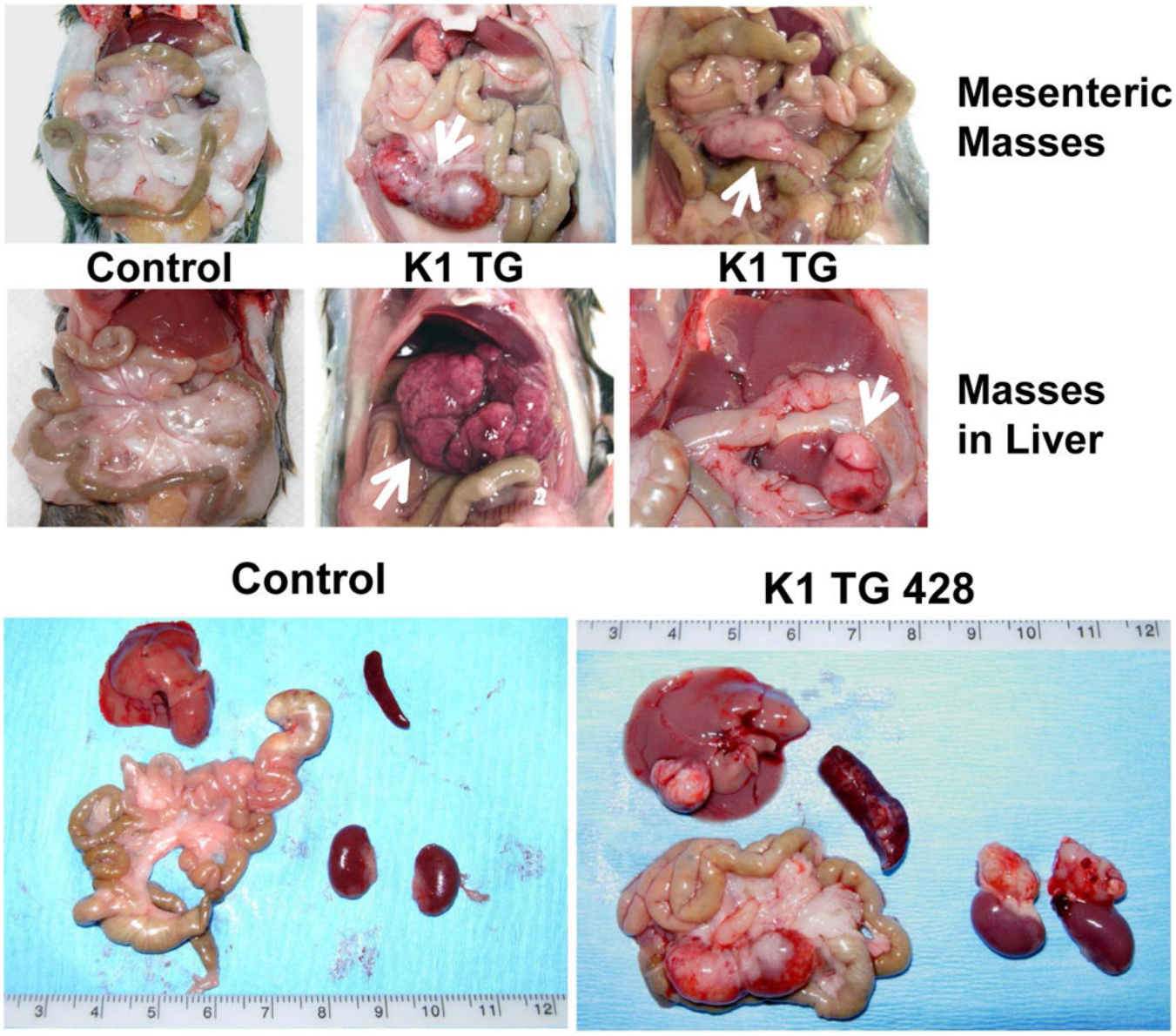

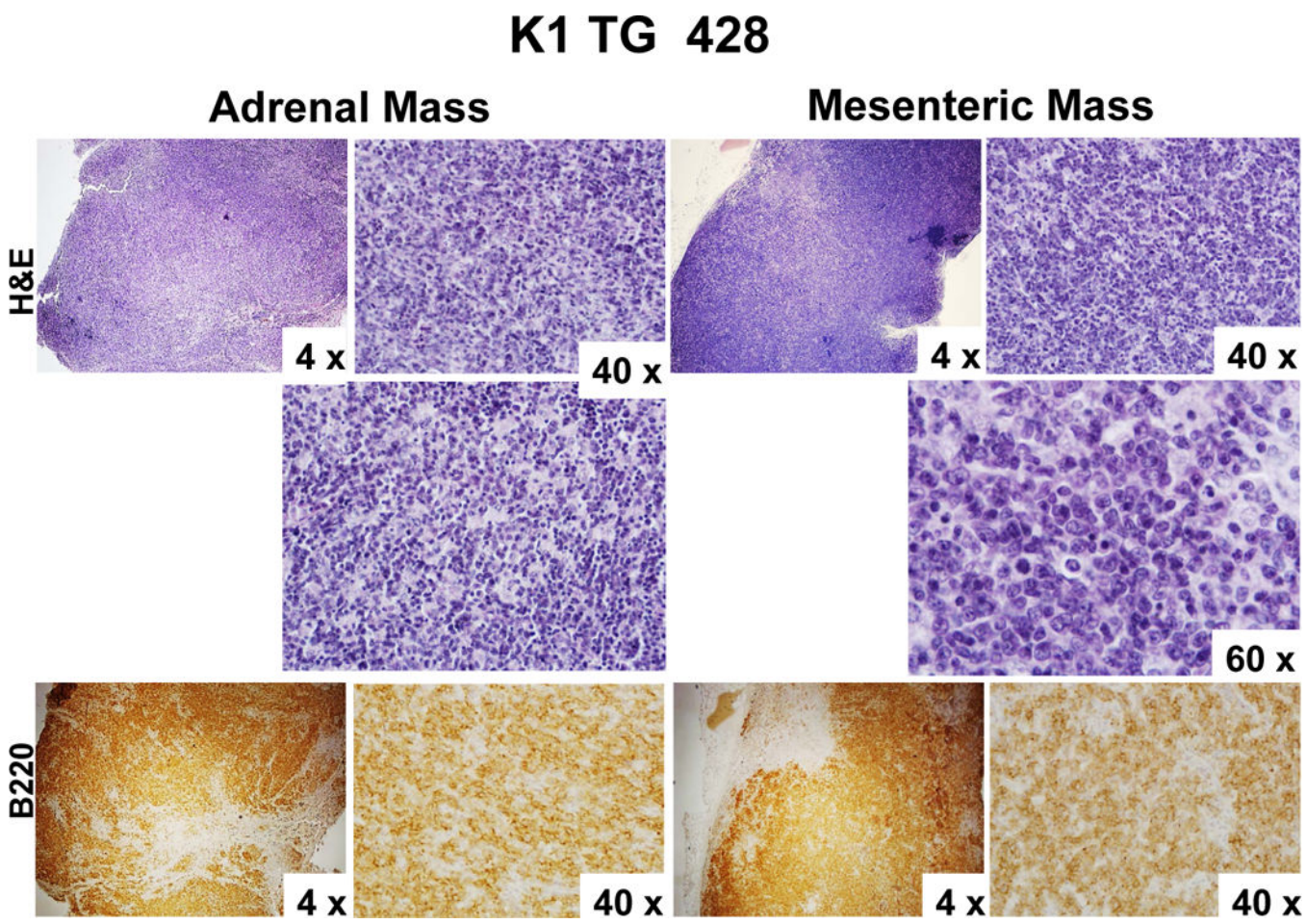

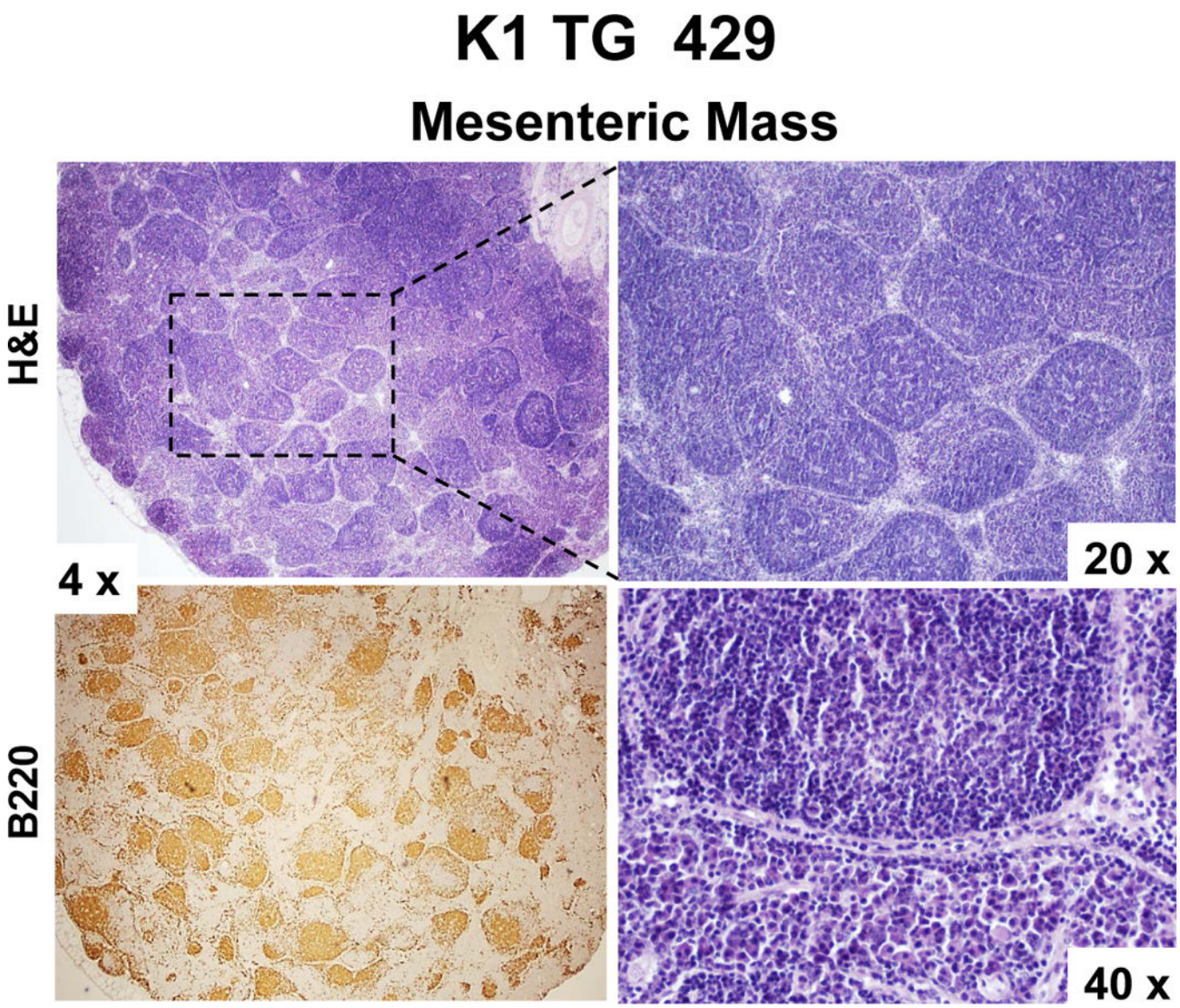

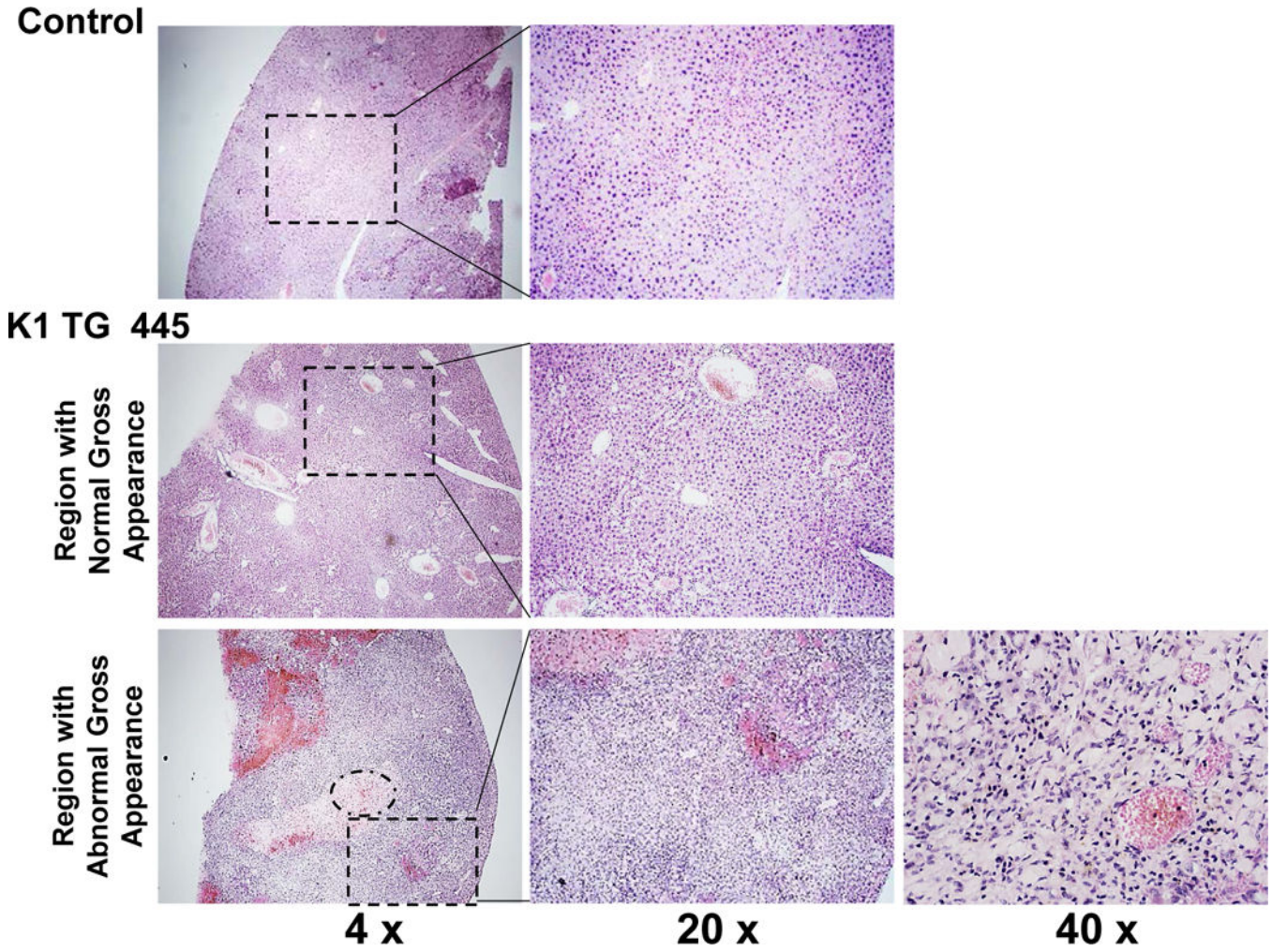

Figure 2. Mesenteric and hepatic tumors in 18 month old K1 transgenic mice

(A) Gross examination of two control (K1-negative littermates) and four K1 transgenic mice with tumors/masses in the mesentery and livers; **(B)** Harvested livers, intestines, spleens and kidneys from control (K1-negative littermate) and K1 transgenic mouse # 428 with tumors/masses in the mesentery, liver, and adrenal glands; **(C)** Hematoxylin/eosin (H&E) and B-cell marker B220 staining of adrenal and mesenteric masses isolated from K1 transgenic mouse # 428; **(D)** H&E and B-cell marker B220 staining of mesenteric mass isolated from K1 transgenic mouse # 429; **(D)** H&E staining of livers from control (K1-negative littermate) and K1 transgenic mouse # 445 showing regions with an abnormal appearance.

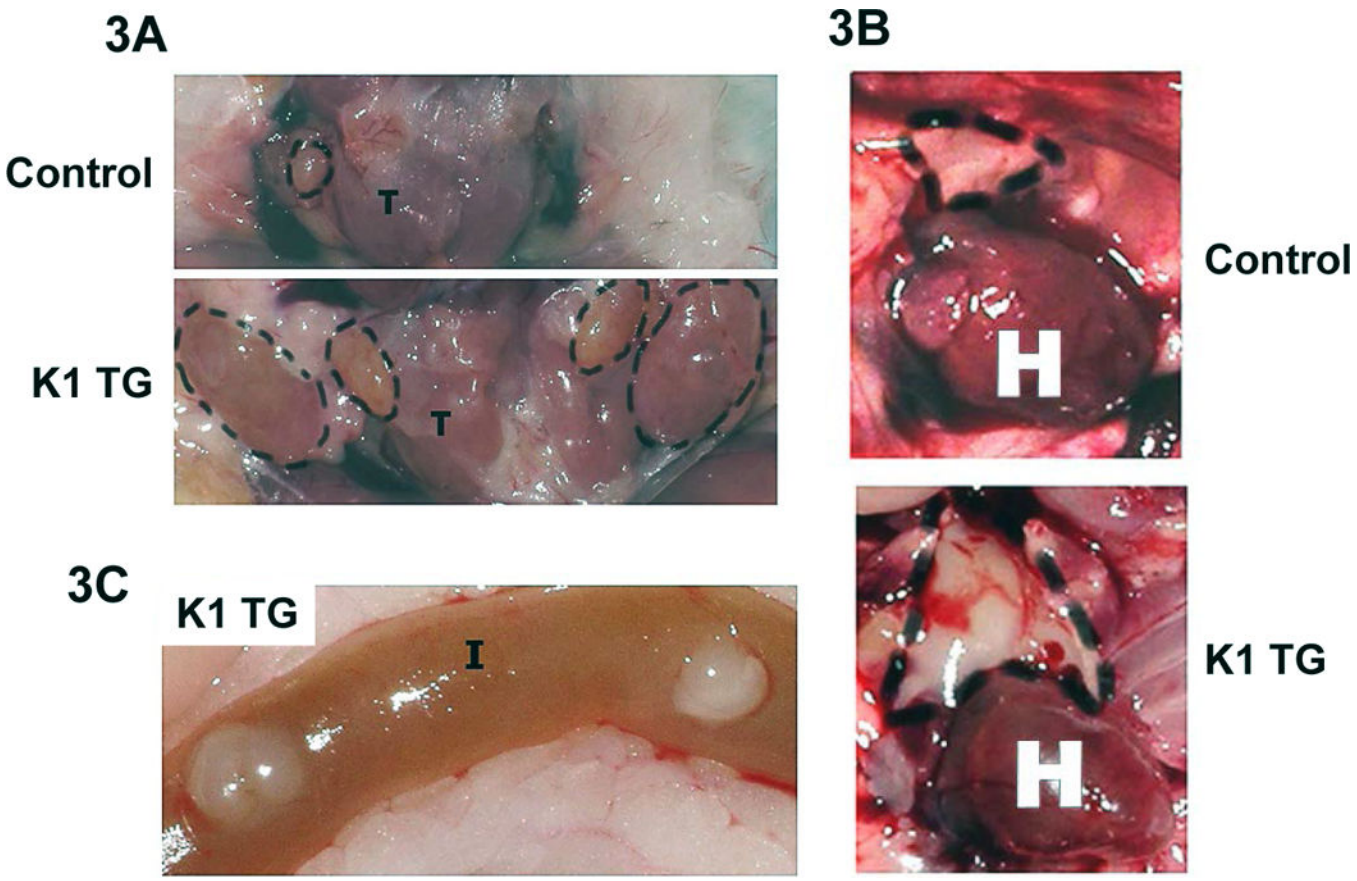

Figure 3. Lymphoid hyperplasia in 8–10 month old K1 transgenic mice

Gross examination of **(A)** cervical lymph nodes and **(B)** thymus from 8 month old control (K1-negative littermate) and K1 transgenic mouse; **(C)** Readily visible Payer's patches in the intestines of K1 transgenic mouse; **(D)** Comparison of spleens from 10 month old K1 transgenic mice and controls (K1-negative littermates).

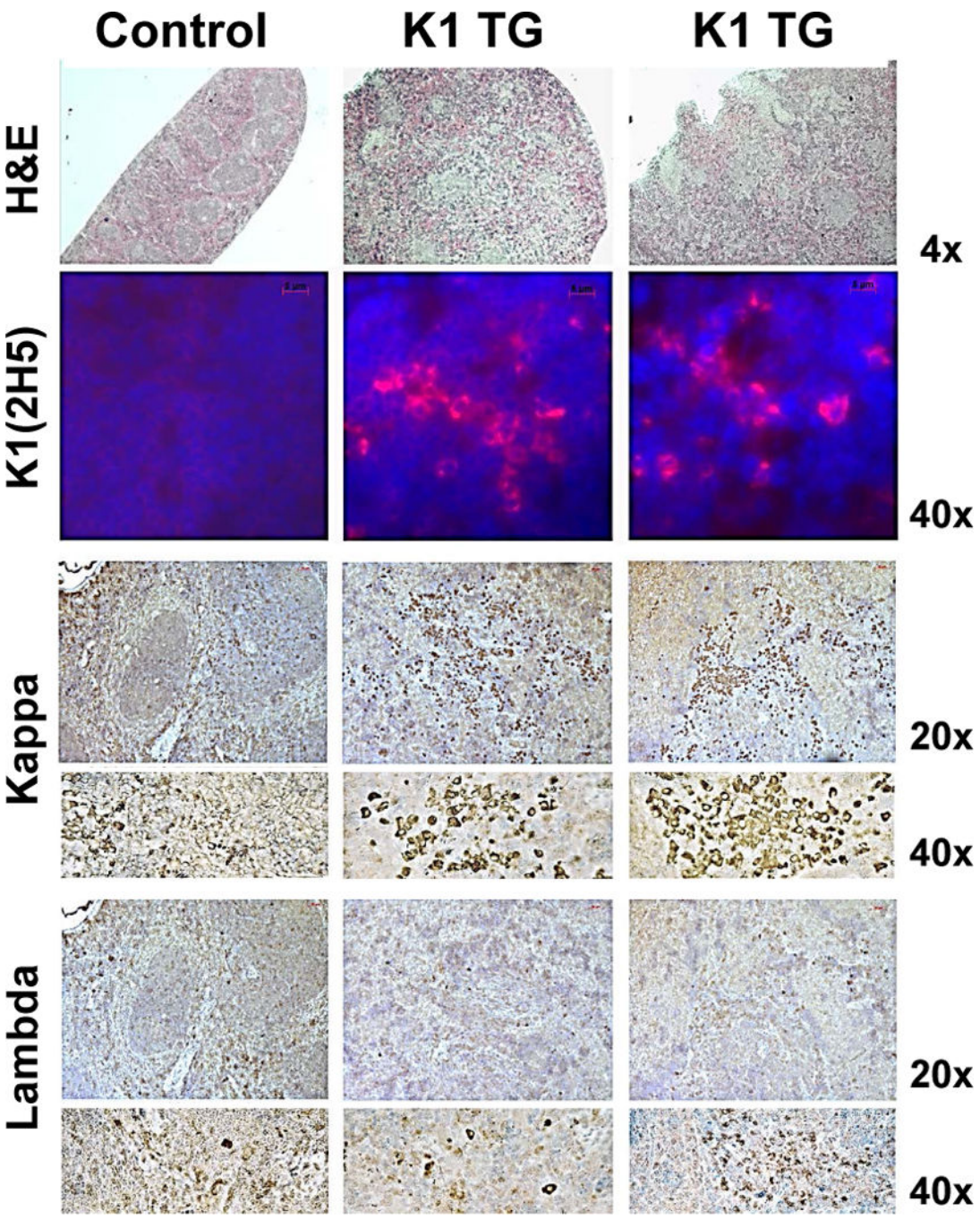

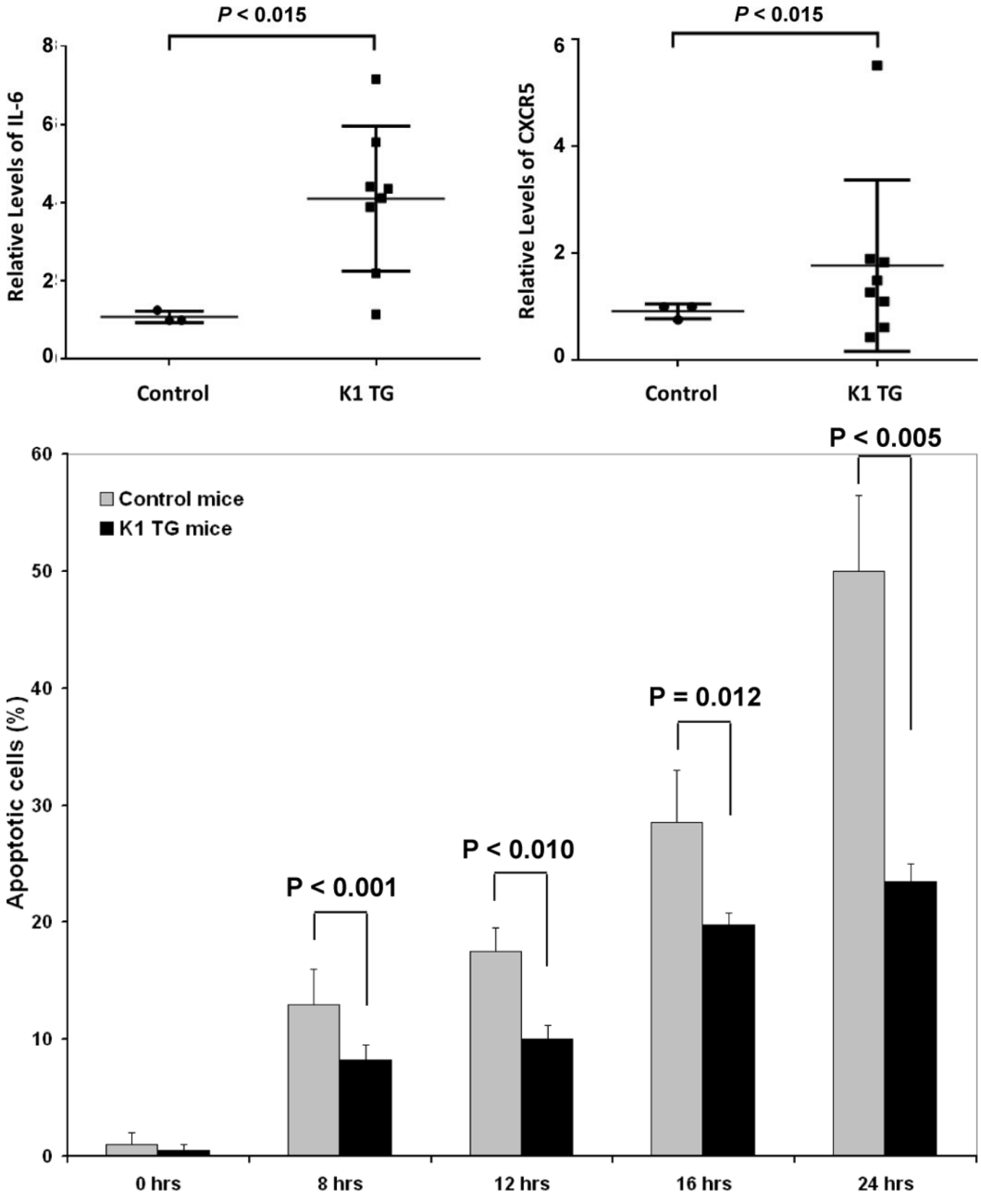

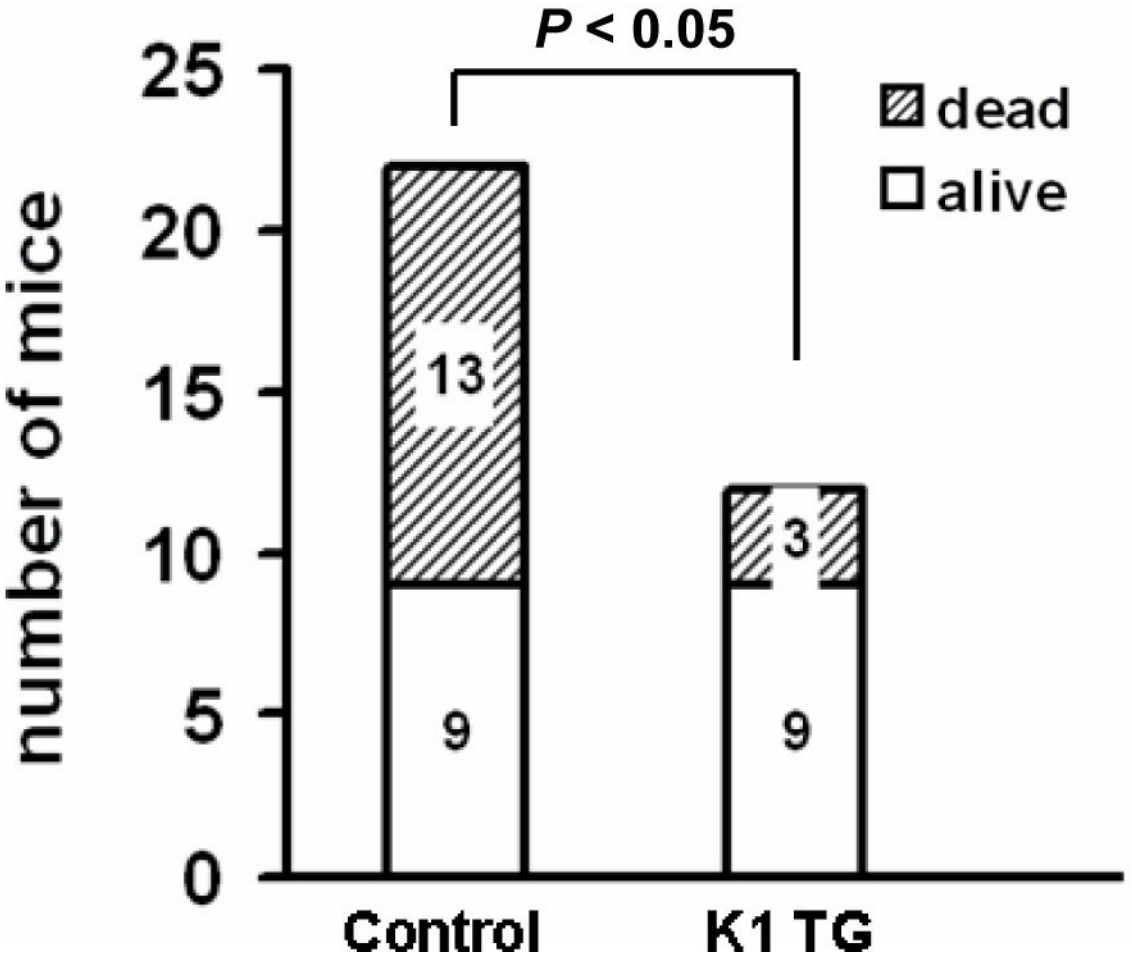

Figure 4. Splenomegaly with expansion of B-cells and resistance to Fas mediated apoptosis in splenocytes and livers of K1 transgenic mice

(A) Hematoxylin/eosin (H&E) staining and immunohistochemistry staining of K1and kappa/lambda light chains in spleens from one control (K1-negative littermate) and two K1 transgenic mice; notable are clusters of kappa-positive and scattered single lambda-positive cells; **(B)** IL-6 (left panel) and CXCR5 (right panel) mRNA levels were analyzed by qRT-PCR in splenic cells isolated from control WT (n=2) and K1-transgenic (n=10) mice; 2 control samples were pooled together; IL-6 average level 4.07 relative to controls (range 1.15 – 7.16); CXCR5 average level 1.24 relative to controls (range 0.62–1.90); **(C)** Splenocytes from 6 month old K1 transgenic mice and control K1-negative littermates were harvested and incubated with 50 ng/mL of anti-Fas antibody Jo2 for the indicated times. Subsequently, cells were analyzed for apoptosis; **(D)** K1 transgenic mice and their K1-negative littermates were challenged with a lethal dose of anti-Fas antibody Jo2 and monitored for survival up to 6 hours post challenge.

Table 1

Tissue pathology

Mouse #	Lymph Nodes (LN)	Spleen (Weight)	Mass/Tumor	Diagnosis
414	A lot of vasculature with perivascular lymphocyte accumulation; secondary follicles forming around perivascular lymphoid sheet	Preserved architecture (120mg)	None	Lymphoid hyperplasia
424	Many secondary follicles	Splenic architecture not disrupted, appears less well defined probably due to staining contrast (130 mg)	Liver mass - appears to be a normal liver tissue with few lymphoid aggregates	Lymphoid hyperplasia
428	Atypical morphology with loss of architecture: atypical cells, signs of apoptosis	Disrupted architecture - expansion of white pulp; large atypical lymphocytes with frequent mitosis and apoptosis (300 mg)	Liver mass - abscess within normal liver tissue; Mesenteric mass - lymphoma tissue, no architecture, increased cellularity, enlarged cells, mitosis; Adrenal mass - lymphoma tissue	Multifocal Lymphoma
429	Tightly packed follicles increased in numbers, only some secondary follicles; plasmacytoid-like cells in between follicles	Disrupted architecture - loss of white/red pulp separation; presence of large atypical cells (430 mg)	Mesenteric mass - lymph node with B-cell nodules	B-cell lymphoma with nodular pattern
437	Lymphoid architecture effaced, secondary follicles present but not prominent; increased plasma cells but no atypical large cells present	Disrupted architecture - loss of white/red pulp separation; presence of large atypical cells, granulocytes (1000 mg)	Abdominal mass - squamous cyst with abscess	Suspicion of lymphoma
444	Normal	Normal appearance (180 mg)	None	
445	Small secondary follicles in mesenteric LN; prominent vasculature with perivascular lymphoid sheet - secondary follicles forming around vessels in cervical LN	*Similar to glycogen storage disorder, no lymphoma-related changes (170 mg)*	Regions of abnormally looking liver tissue contain dividing spindle-like cells and increased vasculature	Lymphoid hyperplasia; angiosarcoma in the liver
470	Effaced secondary follicles in the center of the LN	Normal appearance (80 mg)	None	Lymphoid hyperplasia